

TRADE OFF STUDIES ON WING MANEUVER LOAD ALLEVIATION STRATEGIES BASED ON AILERONS AND WINGLETS MOVABLE SURFACES

Rosario Pecora¹

¹University of Naples "Federico II", Industrial Engineering Department – Aerospace Division

Abstract

Wing load alleviation is a critical aspect of aircraft design aimed at enhancing structural efficiency and safety. This engineering strategy focuses on mitigating aerodynamic stresses on the wings during various flight conditions, such as maneuvers and turbulence. By adopting innovative technologies, including dedicated movable surfaces, engineers seek to reduce bending moments and shears on the wings, with the ultimate goal of minimizing the structural weight.

In this work, a reference civil transportation aircraft was considered as application framework for multidisciplinary trade off studies on ailerons- and winglet-based load alleviation strategies, aiming at:

- Investigating the efficacy of the strategies in terms of achievable reductions in wing bending moment (and shear) at a relevant design condition of the flight envelope for different geometrical settings of alleviator surfaces.
- Assessing the implications induced by such reductions on wing structure sizing and, consequently, on wing mass and wing aeroelastic behavior.

Alleviation strategies have been investigated across a wide range of alleviator geometrical settings. Trends of significant parameters measuring the impacts of load alleviation on wing elastic and inertial properties have been identified, and indications of the benefits and drawbacks of each strategy have been provided based on these findings.

Keywords: Maneuver load alleviation, ailerons, winglet, structural resizing, flutter

1. Introduction

Maneuver load alleviation (MLA) has been a focal point in aerospace research, aiming to mitigate structural stresses during dynamic flight maneuvers and, to some extents, to reduce airframe weight [1]. McRuer et al. [2] have emphasized the critical role of MLA systems in ensuring aircraft safety and longevity. Ravindra [3] and Stevens [4] focused on advanced control algorithms and aerodynamic principles to actively manage loads on aircraft structures thus setting the stage for understanding the multidisciplinary nature of MLA research, integrating aerodynamics, controls, and structural dynamics. In this work, quasi-static maneuver load alleviation is addressed, and the focus is shifted to quantifying the efficacy of various alleviators in reducing wing loads, as well as the potential impact that different alleviation strategies may have on the structural weight of the wing, and ultimately, on its aeroelastic stability.

More specifically, sensitivity analyses have been conducted regarding maneuver load alleviation strategies that utilize movable surfaces such as ailerons and/or winglets as alleviators, aiming to:

- Investigate the efficacy of the strategies in reducing wing bending moment (and shear) under different geometrical settings of alleviator surfaces, and referring to limit design conditions of the flight envelope.
- Examine the implications of these reductions on wing structure sizing, consequentially affecting wing mass and aeroelastic behavior.

The investigated load alleviation strategies differ only in the type of movable surfaces used as alleviators; however, the alleviator control system is assumed to be consistent across each strategy, operating based on measured flight speed and aircraft load factor at the aircraft center of gravity.

Specifically:

- At the limit load factor (n_{lim}) and dive speed (V_D), the system symmetrically rotates alleviator surfaces by an angle ($\beta=\beta^*$) to reduce wing bending moment at the wing root by a desired factor K
- At unitary load factor and cruise speed (V_c), the system remains inactive ($\beta = 0^\circ$).
- At a given load factor n and flight speed V, the system adjusts alleviator surfaces symmetrically by an angle β , determined by a linear function f(n,V), such that f(1,VC) = 0 and $f(n_{lim},V_D) = \beta^*$.

Based on these assumptions, the condition defined by $n = n_{lim}$, $V = V_D$ serves as the reference flight condition for trade-off studies on load alleviation strategies, as it dictates the dimensioning of the load alleviation system.

Trade-off studies were conducted following a conceptual approach encompassing three phases:

- Phase 1 Preliminary sensitivity analysis on the efficacy of alleviation strategies in correspondence of variable geometrical settings of the alleviators (ailerons and/or winglets movable surfaces).
- Phase 2 Identification of optimal alleviator settings for each alleviation strategy.
- Phase 3 Analysis of the effects induced by load alleviation strategies—integrating the optimal settings of alleviators—on wing structure and wing aeroelastic behavior.

A general description of the reference aircraft used for the assessment of the load alleviation strategies has been given in paragraph 2. In paragraph 3 the variable parameters of the trade-off studies have been introduced thus providing a thorough overview of the configuration cases explored for each load alleviation strategy. Paragraphs 4,5 and 6 have been dedicated to the analysis phases 1,2 and 3 respectively, covering the methodologies adopted and the results obtained.

2. Reference aircraft and trade-off studies assumptions

The open rotor configuration investigated within the framework of the low noise domain of the Clean Sky Regional Aircraft program [5] was selected as the investigation platform to address trade-off studies on wing load alleviation strategies. The aircraft (Figure 1a) is characterized by a rear-engine installation and a natural laminar flow wing optimized to ensure high aerodynamic efficiency throughout the entire flight path and to reduce aerodynamic noise during the climb and descent phases. With a capacity of 130 passengers, the aircraft has a Maximum Take-Off Weight (MTOW) ranging from 30,000 kg to 50,000 kg depending on the specific inertial configuration, a limit positive load factor of 2.5, and a dive speed of nearly 170 m/s (Figure 1b).

For trade-off study purposes, the MTOW was set to 40,000 kg, and the center of gravity was considered to be located at the maximum forward position, namely at 21% of the wing mean aerodynamic chord. Load alleviation strategies were investigated with reference to symmetric maneuvers only, allowing for the generation of aerodynamic and structural models covering the right part of the aircraft only.



Figure 1a - Reference Aircraft layout.

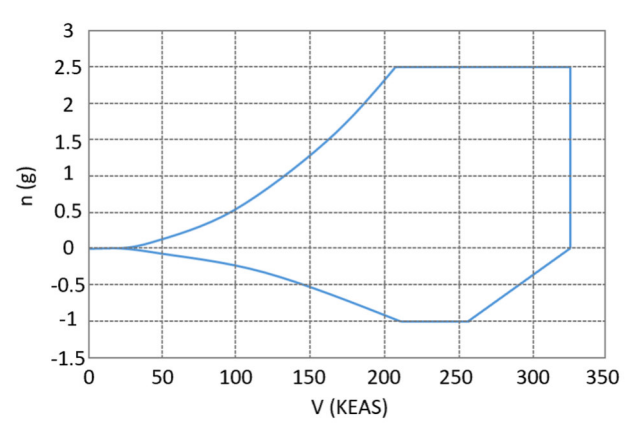


Figure 1b - Reference aircraft maneuvering diagram.

3. Load alleviation strategies, trade-off parameters and analysis cases

The investigated load alleviation strategies differ only based on the movable surfaces used as alleviators. Three strategies were considered, as reported in Table 1.

| STRATEGY ID | ALLEVIATOR | | | | |
|-------------|--|--|--|--|--|
| S1 | Ailerons | | | | |
| S2 | Winglets movable surfaces | | | | |
| S3 | Ailerons and winglets movable surfaces | | | | |

Table 1 - Investigated load alleviation strategies.

Sensitivity analyses were carried out to evaluate the efficacy of each alleviation strategy in correspondence with different geometrical settings of the alleviator. The variable geometrical parameters and their assumed ranges are summarized in Table 2 while the non-variable geometrical parameters and their assumed values are summarized in Table 3. The parameters defining the winglet shape were obtained by similarity with existing aircraft in the same category as the reference aircraft.

Table 2 – Variable geometrical parameters of alleviator surfaces.

| ALLEVIATOR | VARIABLE GEOMETRICAL | RANGE OF VARIABLE PARAMETER | | |
|-------------------------|--|-----------------------------|------|------|
| ALLEVIATOR | PARAMETER | START | STEP | END |
| Aileron | Aileron inboard station position as percent of wing semi-span | 60% | 10% | 70% |
| Alleron | Aileron outboard station position as percent of wing semi-span | 85% | 5% | 100% |
| Winglet movable surface | Winglet Cant angle | 25° | 20° | 85° |

Table 3 – Fixed geometrical parameters of alleviator surfaces.

| ALLEVIATOR | NOT VARIABLE PARAMETER | | ASSUMED VALUE |
|----------------------------|--|-------------|-----------------------------------|
| Aileron | Position of hinge axis as percent of wing local chord | | 80% |
| | Position of hinge axis as percent of winglet local chord | | 80% |
| Minorlat many abla | Span | | Equal to winglet span |
| Winglet movable surface | Winglet shape | Base chord | 2.042 m (equal to wing tip chord) |
| Surface | | Taper ratio | 0.224 |
| | | Sweep angle | 26.62° |
| | | Span | 2.3 m |

Parameters defining winglet shape have been obtained by similitude with already existing aircraft in the same category of the reference one.

By changing the values of the variable geometrical parameters of the alleviators, 44 configuration cases were obtained and investigated to assess the efficacy of each alleviation strategy (Table 4).

For each of the 32 cases related to strategy S3, the winglet movable surface rotation ($\beta_{\text{(wms)}}$) was assumed to be dependent on the aileron deflection ($\beta_{\text{(aileron)}}$) with a gearing factor γ defined as:

$$\gamma = \frac{\beta_{(wms)}}{\beta_{(aileron)}}$$

The gearing factor was considered as an additional trade-off parameter and was varied within the range [0, 1].

Table 4 - Investigated cases for trade off analyses on the efficacy of load alleviation strategies.

| | | | | ALLEVIATOR GEOMETRICAL SETTING | | |
|----------------------------|-------------------------------|-----------------|-------------------------|--|------------------|---------------------------|
| ALLEVIATION STRATEGY ID | | USED ALLEVIATOR | | AILERON | | WINGLET MOV. SURFACE |
| \downarrow | CASE ID | AILERON | WINGLET MOV. SURFACE | η_{in} | η _{out} | WINGLET CANT ANGLE [°] |
| | Case_A1 | • | | 70% | 85% | - |
| | Case_A2 | • | | 70% | 90% | - |
| | Case_A3 | • | | 70% | 95% | - |
| S1 | Case_A4 | • | | 70% | 100% | - |
| 31 | Case_B1 | • | | 60% | 85% | - |
| | Case_B2 | • | | 60% | 90% | - |
| | Case_B3 | • | | 60% | 95% | - |
| | Case_B4 | • | | 60% | 100% | - |
| | Case_W25M | | • | - | - | 25 |
| S2 | Case_W45M | | • | - | - | 45 |
| 32 | Case_W65M | | • | - | - | 65 |
| | Case_W85M | | • | - | - | 85 |
| 62 | Case_ <i>ij</i> _W <i>k</i> M | • | • | Case_ij combined with Case_WkM, where: i = A,B | | |
| S3 | | | | , j | = 1,2,3,4 | |
| | | | | k | = 25,45,6 | 65,85 |
| | <u>LEGEND</u> | | | | | |

 $\eta_{\text{in:}} \quad \text{Position of aileron inboard station as percent of wing semi-span} \\ \eta_{\text{out:}} \quad \text{Position of aileron outboard station as percent of wing semi-span}$

4. Preliminary sensitivity analyses: alleviation strategies efficacy VS alleviator geometrical settings

Specific indices were defined to measure the efficacy of each alleviation strategy and the effects induced on it by changes in alleviator geometry (Table 5).

Table 5 – Efficacy indices formulation.

| | LOAD ALLEVIATION STRATEGY | EFFICACY INDEX (ηall) | | | |
|--|--|---|--|--|--|
| | S1 (Aileron as unique load alleviator) | $\eta_{all} = rac{\widetilde{M}_{eta(aileron)}}{\widetilde{M}_{lpha} + \widetilde{M}_{0}}$ | | | |
| (Wing | S2 et movable surface as unique load alleviator) | $oldsymbol{\eta}_{all} = rac{\widetilde{M}_{eta(wms)}}{\widetilde{M}_{lpha} + \widetilde{M}_{0}}$ | | | |
| (Aileron and winglet movable surface as load alleviators) $\eta_{all} = \frac{\widetilde{M}_{\beta(aileron)} + \gamma \widetilde{M}_{\alpha}}{\widetilde{M}_{\alpha} + \widetilde{M}_{0}}$ | | | | | |
| $\frac{\textbf{LEGEND}}{\widetilde{M}_{\beta(aileron)}}$ | $\widetilde{M}_{\beta(aileron)}$: Bending moment at wing root due only to unitary (negative, i.e. upwards) deflection of the aileron at unitary dynamic pressure. | | | | |
| $\widetilde{M}_{eta(\mathit{wms})}$ | | Bending moment at wing root due only to unitary (negative, i.e. upwards) deflection of winglet movable surface at unitary dynamic pressure. | | | |
| γ | γ : Winglet movable surface-Aileron gear factor (γ =(Winglet movable surface deflection / Aileron deflection), γ \in [0:1]). | | | | |
| \widetilde{M}_{lpha} | \tilde{I}_{α} : Bending moment at wing root due only to unitary A/C (positive) incidence angle at unitary dynamic pressure. | | | | |
| ${\widetilde M}_0$ | \widetilde{M}_0 : Bending moment at wing root related at zero incidence and unitary dynamic pressure. | | | | |

Although the formulation used is based on bending moments due only to unitary effects, it is evident that all parameters provide a rough measurement of each strategy's capability in alleviating wing bending moments.

Efficacy indices have been evaluated for all the alleviator configuration cases reported in Table 4.

For each alleviator configuration case, unitary bending moments were obtained by vortex lattice method (VLM, [6]). To cover all possible configurations, five different aerodynamic models were generated. The models (Figure 2) covered only the right wing and horizontal tail and were characterized by nine panels (eight for the wing and one for the horizontal tail) for cases A1-A4 and B1-B4. An additional panel with four different cant angles was included to account for the presence of the winglet in the configuration cases related to strategies S2 and S3 (see Table 4). All the panels were meshed into an adequate number of boxes to properly account for the aerodynamic effects induced by the deflection of the movable surface.

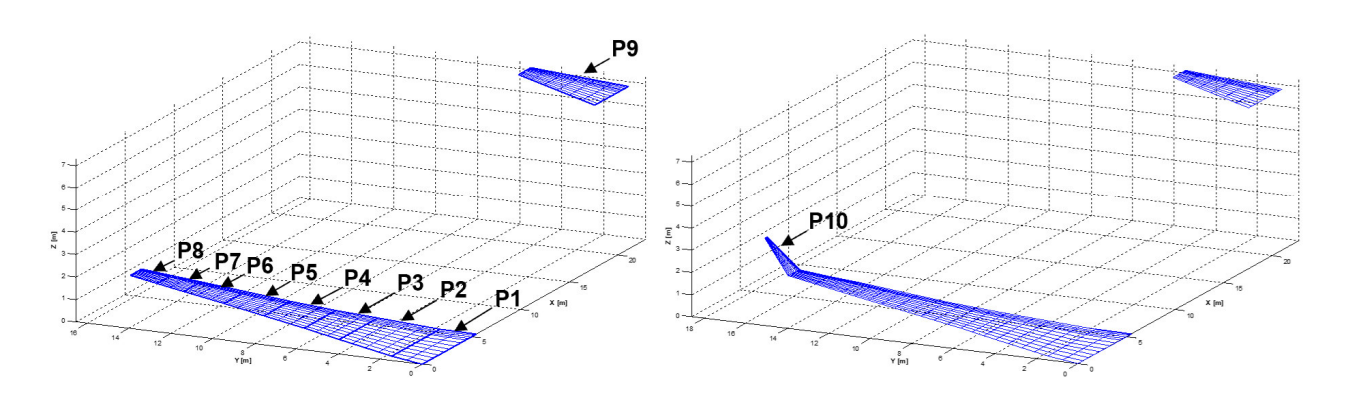


Figure 2 – Aircraft aerodynamic for the load alleviation strategies S1 (left) and S2,S3 (right).

In Figures 3, 5 and 6, η_{all} has been plotted against the alleron outboard station position along the wing span for all the alleviator configuration cases pertaining to strategies S1 and S3. In Figure 4, the efficacy index related to strategy S2 has been plotted against the winglet cant angle.

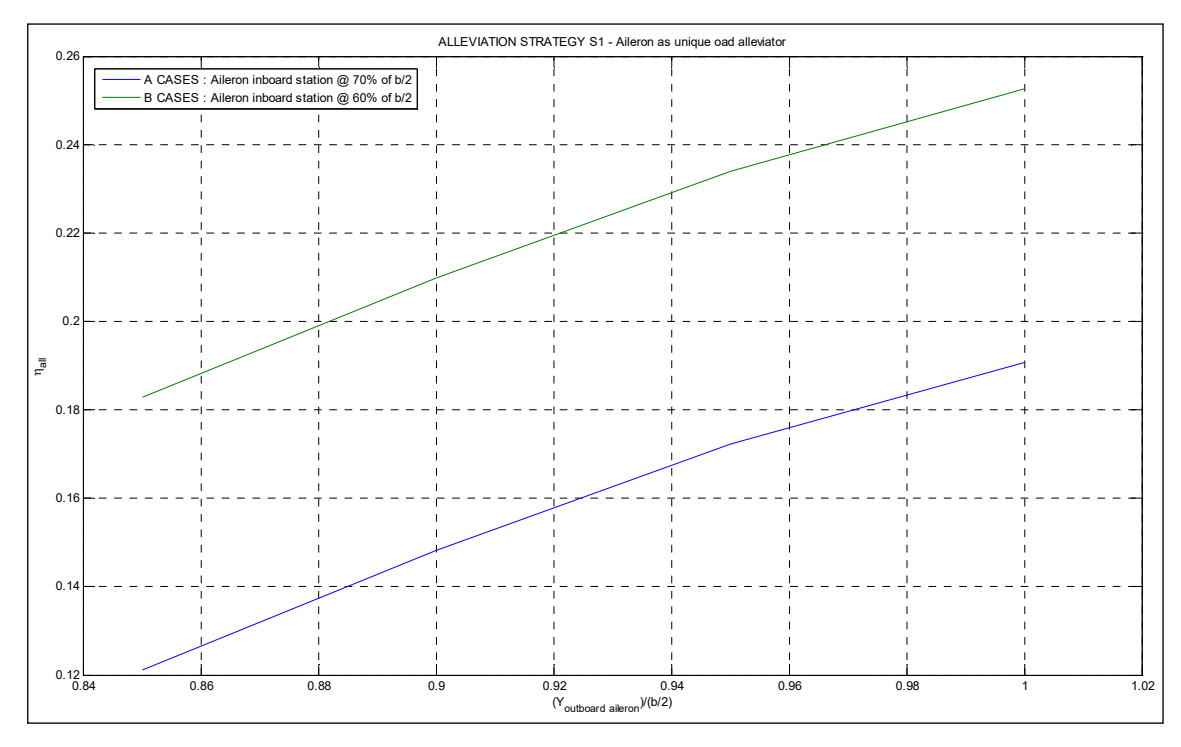


Figure 3 – Efficacy index trends for alleviation strategy S1.

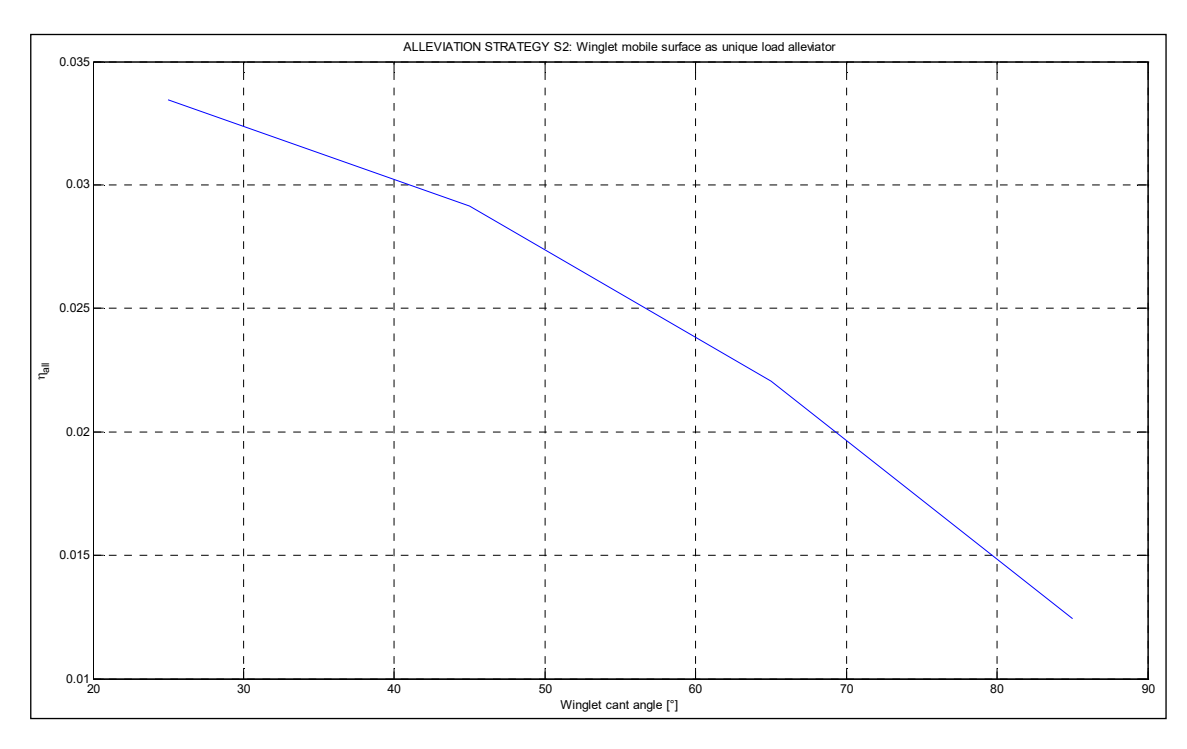


Figure 4 – Efficacy index trends for alleviation strategy S2.

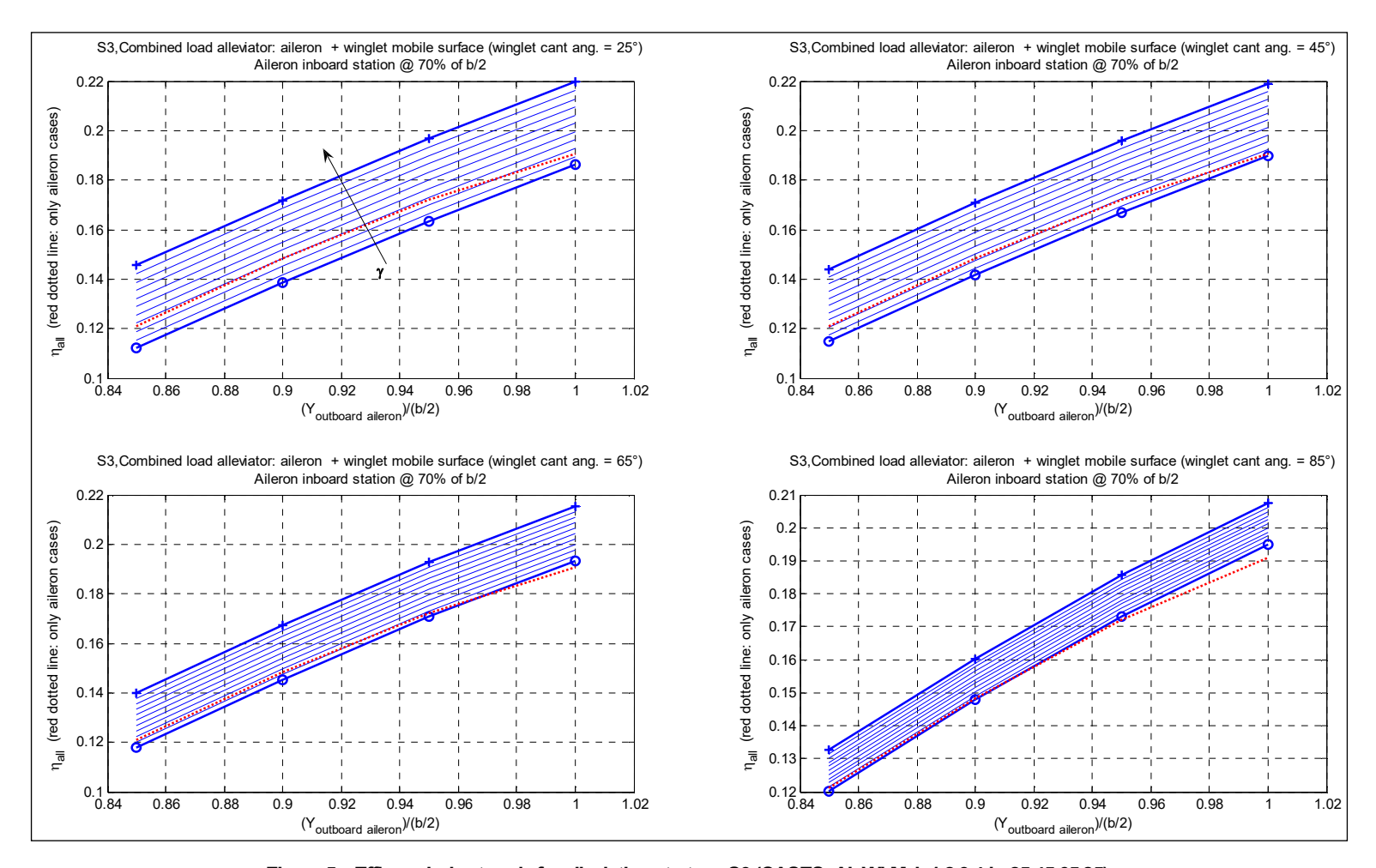


Figure 5 – Efficacy index trends for alleviation strategy S3 (CASES_Aj_WkM, j=1,2,3,4;k=25,45,65,85).

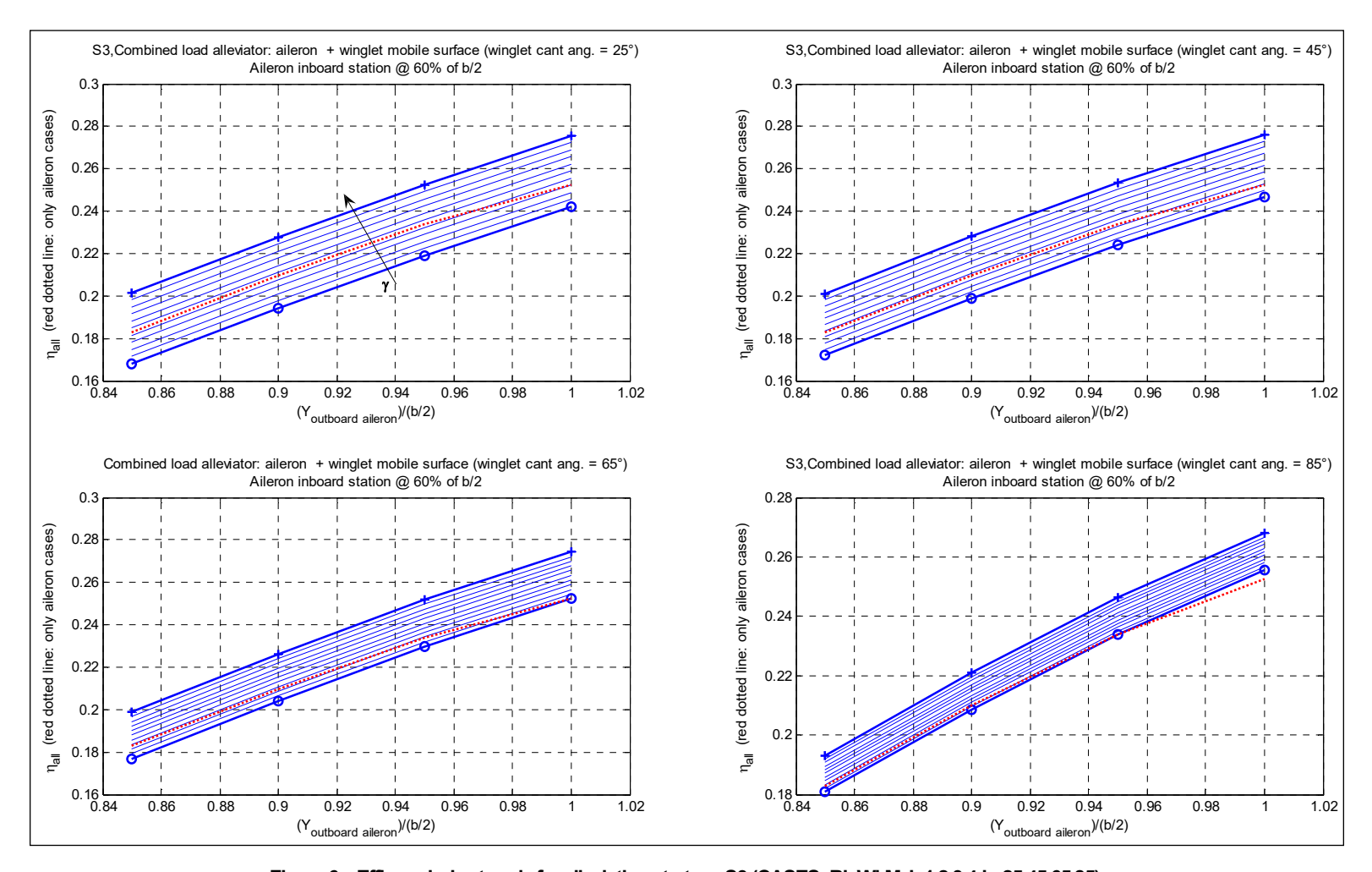


Figure 6 – Efficacy index trends for alleviation strategy S3 (CASES_Bj_WkM, j=1,2,3,4;k=25,45,65,85).

Referring to Figure 3, it can be observed that increases in aileron span lead to higher alleviation efficacy. Moreover, the trend curve related to B cases is shifted compared to the one related to A cases due to the aerodynamic contribution in bending moment alleviation from the aileron boxes positioned between 60% and 70% of the wing semispan

From Figure 4, it can be observed that the efficacy index related to strategy S2 decreases as winglet cant angle increases; such trend finds its explanation in the fact that the arm of the resultant alleviating lift, generated by winglet movable surface negative deflection, diminishes while cant angle increases. Regardless of the winglet cant angle, the efficacy index for strategy S2 is an order of magnitude lower than the average efficacy index for strategies S1 and S3. Therefore, it is clear that to achieve satisfactory alleviation performance, an alleviation strategy based solely on the winglet's movable surface is not recommended.

In Figures 5, 6, η_{all} has been plotted also at different values of γ ranging between 0 and 1; the curves characterized by a circle mark are related to γ =0 while those marked with a '+' symbol are pertinent to γ =1. In order to have a fast visual comparison between strategies S3 and S1, the curves of Figure 3 have been also reported by means of red dotted lines.

Referring to Figures 5,6, the following considerations can then be made:

- 1. Regardless of γ value, the slope of the curves increases as winglet cant angle increases; this is essentially consequence of M_{α} and M_0 trends VS winglet cant angle. While winglet cant angle increases, M_{α} rapidly decreases and M_0 remains quite unchanged thus leading to a reduction in the denominator of the formula defining η_{all} . At a parity of aileron outboard station position, higher efficacy indices may be therefore obtained by increasing winglet cant angle.
- 2. Variations of γ from 0 to 1 just shift trends curves towards higher efficacy index values at a parity of aileron outboard station position. The magnitude of the shift decreases as winglet cant angle increases due to the decay of alleviating bending moment induced by winglet movable surface (see Figure 4). As a consequence of what observed at point 1, more γ is needed to obtain a desired efficacy index as winglet cant angle decreases at a parity of aileron outboard station position. Such circumstance is also highlighted by the position of γ =0 curve with respect to the red dotted line (pertaining to strategy S1) as winglet cant angle increases: at winglet cant angles between 25° and 65° degrees such curve is always below the red dotted line, while for winglet cant angles greater than 65° the curve moves slightly up the red dotted line.
- 3. By the comparing the curves for strategy S3 with those for strategy S1 (red dotted lines), it can be observed that, by properly choosing the value of γ in the range [0,1], an alleviation strategy based on both aileron and winglet movable surfaces as alleviators always achieves higher alleviation performance compared to a strategy using only the aileron, given the same aileron geometrical settings.

5. Individuation of the optimal alleviators' settings for each alleviation strategy

Optimal geometric settings for the alleviators in each of the investigated strategies have been determined based on the values assumed by the rigid aircraft re-trim angles in the presence of load alleviation. For each strategy and alleviator configuration case, the following procedure has been followed.

Step 1

Rigid A/C trim angles in absence of load alleviation were at first calculated by solving the equation set (1) in correspondence of the (symmetric) maneuver parameters recapped in Table6.

$$\begin{cases} \widetilde{C}z_{\alpha} \cdot \overline{\alpha} + \widetilde{C}z_{\delta} \cdot \overline{\delta} &= \frac{ACM \cdot n_{z} \cdot g}{S_{W} \cdot q} - \widetilde{C}z_{0} \\ \widetilde{C}m_{\alpha} \cdot \overline{\alpha} + \widetilde{C}m_{\delta} \cdot \overline{\delta} &= -\frac{x_{cg} \cdot ACM \cdot n_{z} \cdot g}{S_{W} \cdot q \cdot MAC} - \widetilde{C}m_{0} \end{cases}$$

(1)

Table 6 - Manoeuvre parameters for A/C trim.

| PARAMETER | SYMBOL [UNIT] | ASSUMED VALUE | NOTES |
|----------------------|---------------------|-------------------|---|
| Load factor | n _z [g] | 2.5 | limit load factor |
| A/C Mass | ACM [Kg] | 40000 | A/C MTOW |
| X-position of A/C cg | x _{cg} [m] | @ 21% of wing MAC | |
| Dynamic pressure | q [N/m²] | 16598.59 | Dynamic pressure at V=V _D =164.62 m/s and sea level. |

The symbols used in eq.(1) that are not reported in Table 6 are explained below:

A/C incidence angle, trimmed maneuver without load alleviation.

A/C tail deflection, trimmed maneuver without load alleviation.

 $\widetilde{C}z_{\alpha},\widetilde{C}z_{\delta},\widetilde{C}z_{0}$ Rigid A/C aerodynamic derivatives at unitary dynamic pressure (unitary derivatives). Moment coefficients are referred to Y-axis of aerodynamic system.

 S_w Wing surface area.

Step 2

By using the values $\overline{\alpha}$ and $\overline{\delta}$ coming from step 1, the bending moment at wing root has been evaluated in correspondence of the trimmed condition without load alleviation:

$$M_{off} = \left(\widetilde{M}_{\alpha} \cdot \overline{\alpha} + \widetilde{M}_{\delta} \cdot \overline{\delta} + \widetilde{M}_{0}\right) \cdot q \tag{2}$$

where \widetilde{M}_a and \widetilde{M}_0 represent the unitary bending moments already defined in previous paragraph, and \widetilde{M}_{δ} the bending moment at wing root induced by unitary A/C tail deflection at unitary dynamic pressure.

An alleviation factor K has then be defined according to the following equation :

$$K = 1 - \frac{M_{on}}{M_{off}} \tag{3}$$

where M_{on} the desired bending moment at wing root in trimmed condition and in presence of load alleviation.

The alleviation factor K was assumed to vary in the range R=[0:0.25]; for each value $K_i \in R$, rigid A/C re-trim angles α,δ have been evaluated together with the alleviator deflection β required to achieve the alleviation factor K_i. Re-trim angles and alleviator deflections have been calculated by the solution of the eq.s (4),(5) and (6) for alleviator configuration cases of strategies S1,S2 and S3 respectively.

$$\begin{cases}
\widetilde{C}z_{\alpha} \cdot \alpha + \widetilde{C}z_{\delta} \cdot \delta + \widetilde{C}z_{\beta(aileron)} \cdot \beta_{(aileron)} &= \frac{ACM \cdot n_{z} \cdot g}{S_{W} \cdot q} - \widetilde{C}z_{0} \\
\widetilde{C}m_{\alpha} \cdot \alpha + \widetilde{C}m_{\delta} \cdot \delta + \widetilde{C}m_{\beta(aileron)} \cdot \beta_{(aileron)} &= -\frac{x_{cg} \cdot ACM \cdot n_{z} \cdot g}{S_{W} \cdot q \cdot MAC} - \widetilde{C}m_{0} \\
\widetilde{M}_{\alpha} \cdot \alpha + \widetilde{M}_{\delta} \cdot \delta + \widetilde{M}_{\beta(aileron)} \cdot \beta_{(aileron)} &= (1 - K_{i})M_{off} - \widetilde{M}_{0}
\end{cases}$$
(4)

$$\begin{cases}
\widetilde{C}z_{\alpha} \cdot \alpha + \widetilde{C}z_{\delta} \cdot \delta + \widetilde{C}z_{\beta(wms)} \cdot \beta_{(wms)} &= \frac{ACM \cdot n_{z} \cdot g}{S_{W} \cdot q} - \widetilde{C}z_{0} \\
\widetilde{C}m_{\alpha} \cdot \alpha + \widetilde{C}m_{\delta} \cdot \delta + \widetilde{C}m_{\beta(wms)} \cdot \beta_{(wms)} &= -\frac{x_{cg} \cdot ACM \cdot n_{z} \cdot g}{S_{W} \cdot q \cdot MAC} - \widetilde{C}m_{0} \\
\widetilde{M}_{\alpha} \cdot \alpha + \widetilde{M}_{\delta} \cdot \delta + \widetilde{M}_{\beta(wms)} \cdot \beta_{(wms)} &= (1 - K_{i})M_{off} - \widetilde{M}_{0}
\end{cases}$$
(5)

$$\begin{cases}
\widetilde{C}z_{\alpha} \cdot \alpha + \widetilde{C}z_{\delta} \cdot \delta + \left(\widetilde{C}z_{\beta(aileron)} + \gamma \cdot \widetilde{C}z_{\beta(wms)}\right) \cdot \beta_{(aileron)} &= \frac{ACM \cdot n_{z} \cdot g}{S_{W} \cdot q} - \widetilde{C}z_{0} \\
\widetilde{C}m_{\alpha} \cdot \alpha + \widetilde{C}m_{\delta} \cdot \delta + \left(\widetilde{C}m_{\beta(aileron)} + \gamma \cdot \widetilde{C}m_{\beta(wms)}\right) \cdot \beta_{(aileron)} &= -\frac{x_{cg} \cdot ACM \cdot n_{z} \cdot g}{S_{W} \cdot q \cdot MAC} - \widetilde{C}m_{0} \\
\widetilde{M}_{\alpha} \cdot \alpha + \widetilde{M}_{\delta} \cdot \delta + \left(\widetilde{M}_{\beta(aileron)} + \gamma \cdot \widetilde{M}_{\beta(wms)}\right) \cdot \beta_{(aileron)} &= (1 - K_{i})M_{off} - \widetilde{M}_{0}
\end{cases}$$
(6)

Eq.s (4),(5),(6) were solved always referring to the maneuver parameters of Table 6.

The symbols used in eq.s (4)-(6) and not already reported in Table 6 have been explained below:

A/C incidence angle, trimmed maneuver with load alleviation.

 δ A/C tail deflection, trimmed maneuver with load alleviation.

 $eta_{ ext{(aileron)}}$ Aileron deflection required to achieve a specified alleviation factor

in trimmed condition.

 $eta_{\scriptscriptstyle (wms)}$ Winglet movable surface deflection required to achieve a

specified alleviation factor in trimmed condition.

 γ $\beta_{(wms)}/\beta_{(aileron)}$ (variable from 0 to 1).

 $\widetilde{C}z_{\beta(ullet)},\widetilde{C}m_{\beta(ullet)}$ Rigid A/C unitary aerodynamic derivatives related to alleviator

deflection $\beta_{(\bullet)}$ (\bullet : *aileron* or *wms*).

 \widetilde{M} Bending moment at wing root induced by unitary (negative)

alleviator deflection at unitary dynamic pressure.

The coefficients of eq.s (4),(5),(6) obviously change according to alleviator configuration cases. The unitary aerodynamic derivatives were evaluated by means of VLM applied to the aerodynamic models developed for the preliminary analysis described in the previous paragraph.

Step 3

The space of eq.s (4),(5),(6) solutions was plotted against the alleviation factor K (K=1-M_{on}/M_{off}) and for eq.s (6) also in correspondence of different values of γ ranging from 0 up to 1.

The following constraints were then imposed to re-trim angle δ and to aileron deflection $\beta_{(aileron)}$ to individuate the optimal alleviator geometrical settings for each of the investigated strategies:

$$\begin{cases} |\delta| \le 5.6^{\circ} \\ |\beta_{(aileron)}| \le 15^{\circ} \end{cases}$$
 (7)

Rational criteria were finally used to select the optimal geometrical setting for the alleviator:

- 1. **Strategy S1(/S2)**, aileron (/winglet movable surface used as alleviator): Configuration leading to the highest values of K under imposed constraints;
- 2. **Strategy S3**, aileron + winglet movable surface used as alleviators: Configuration leading to the highest values of K under imposed constraints and in correspondence of the largest number of γ values within the γ -range.

In Figure 7, achievable alleviation factors under the constraints of eqs. (7) have been plotted for all configuration cases corresponding to strategy S1. According to the defined criteria, CASE_A4 resulted in the optimal configuration case for strategy S1.

This case was chosen as the reference configuration for trade-off studies on the effects induced by load alleviation strategy S1 on wing structure and aeroelastic behavior, as discussed in the following paragraphs.

In Figure 8, the constraints of eq.s (7) have been represented by red-dashed limit curves. It can be observed that strategy S2 is characterized by very low alleviation performance, confirming the conclusions drawn from preliminary analyses presented in the previous paragraph. Therefore, no configuration case related to strategy S2 has been chosen for further trade-off analysis on the impact of alleviation strategy on wing structure and aeroelastic behavior

In Figures 9a and 9b, achievable alleviation factors under the constraints of eqs. (7) have been plotted for all configuration cases belonging to strategy S3, corresponding to γ values ranging from 0 to 1.

Both CASE_A4_W65M and CASE_A4_W85M have been considered to satisfy the selection criteria. Since the winglet arrangement of CASE_A4_W65M is preferable from an aeroelastic standpoint, only this case has been chosen as the reference configuration for trade-off studies on the effects induced by load alleviation strategy S3 on wing structure and aeroelastic behavior.

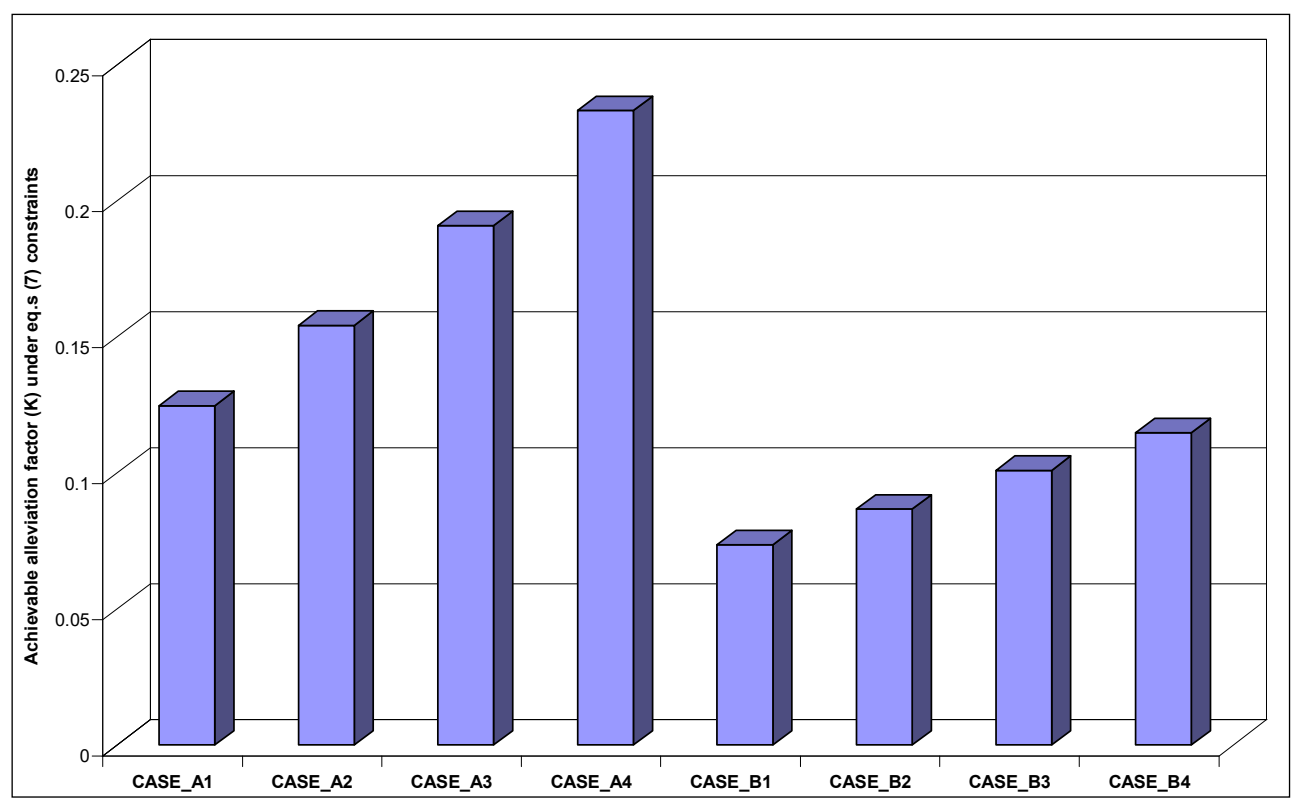


Figure 7 - Alleviation strategy S1: Achievable alleviation factors under eq.s (7) constraints.

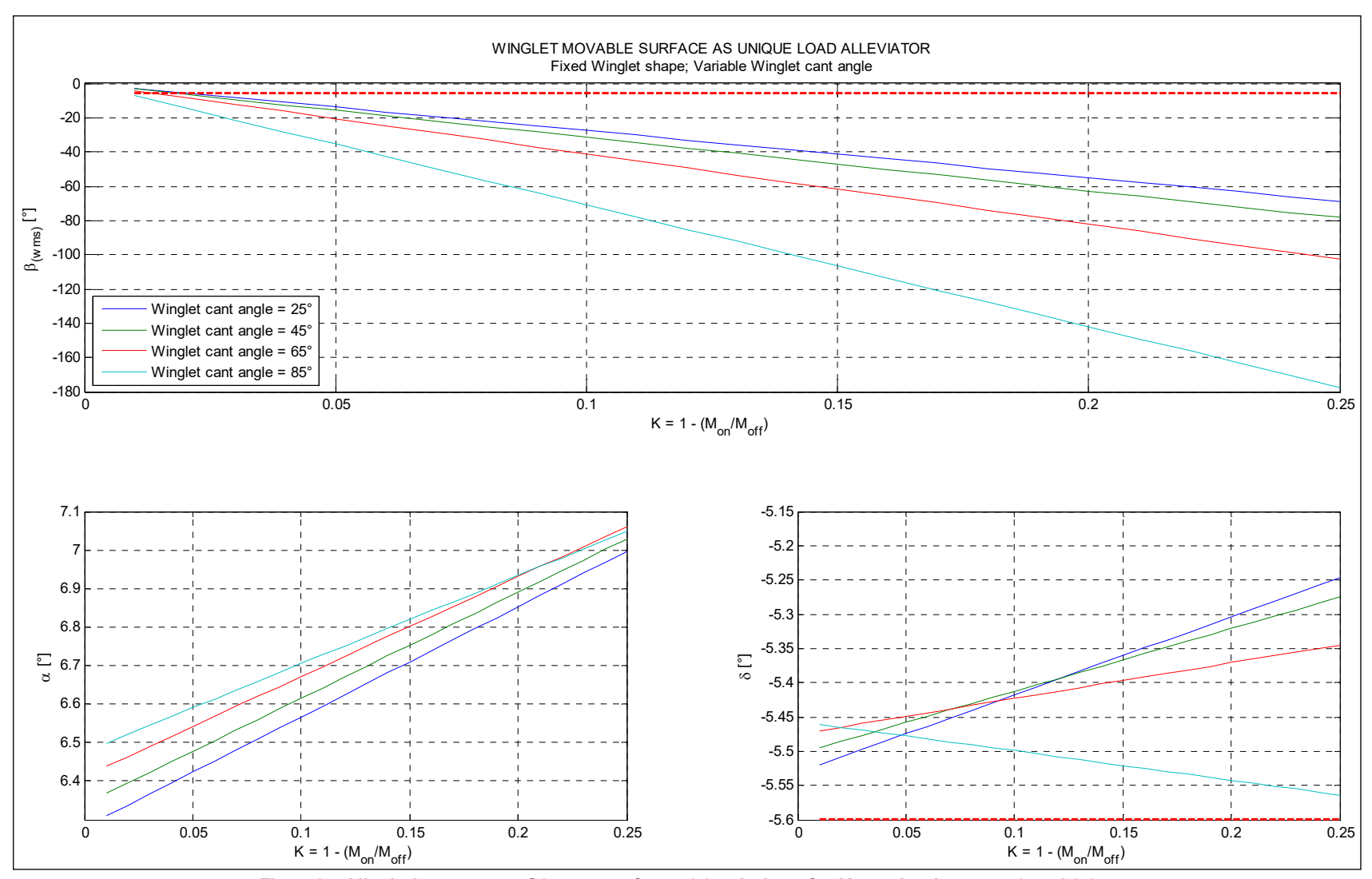


Figure 8 – Alleviation strategy S2: space of eq.s (5) solutions for K ranging between 0 and 0.25.

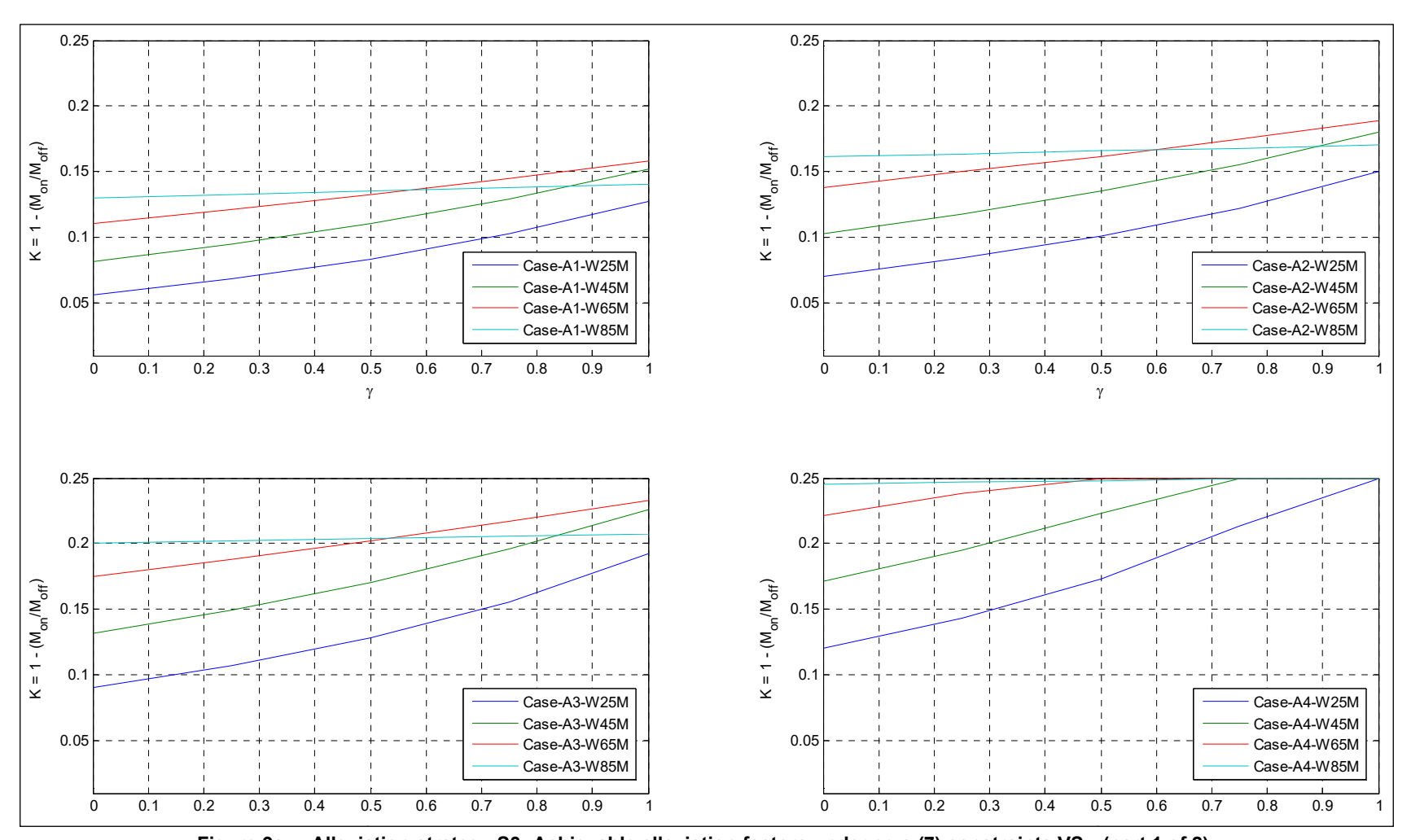


Figure 9a – Alleviation strategy S3: Achievable alleviation factors under eq.s (7) constraints VS γ (part 1 of 2).

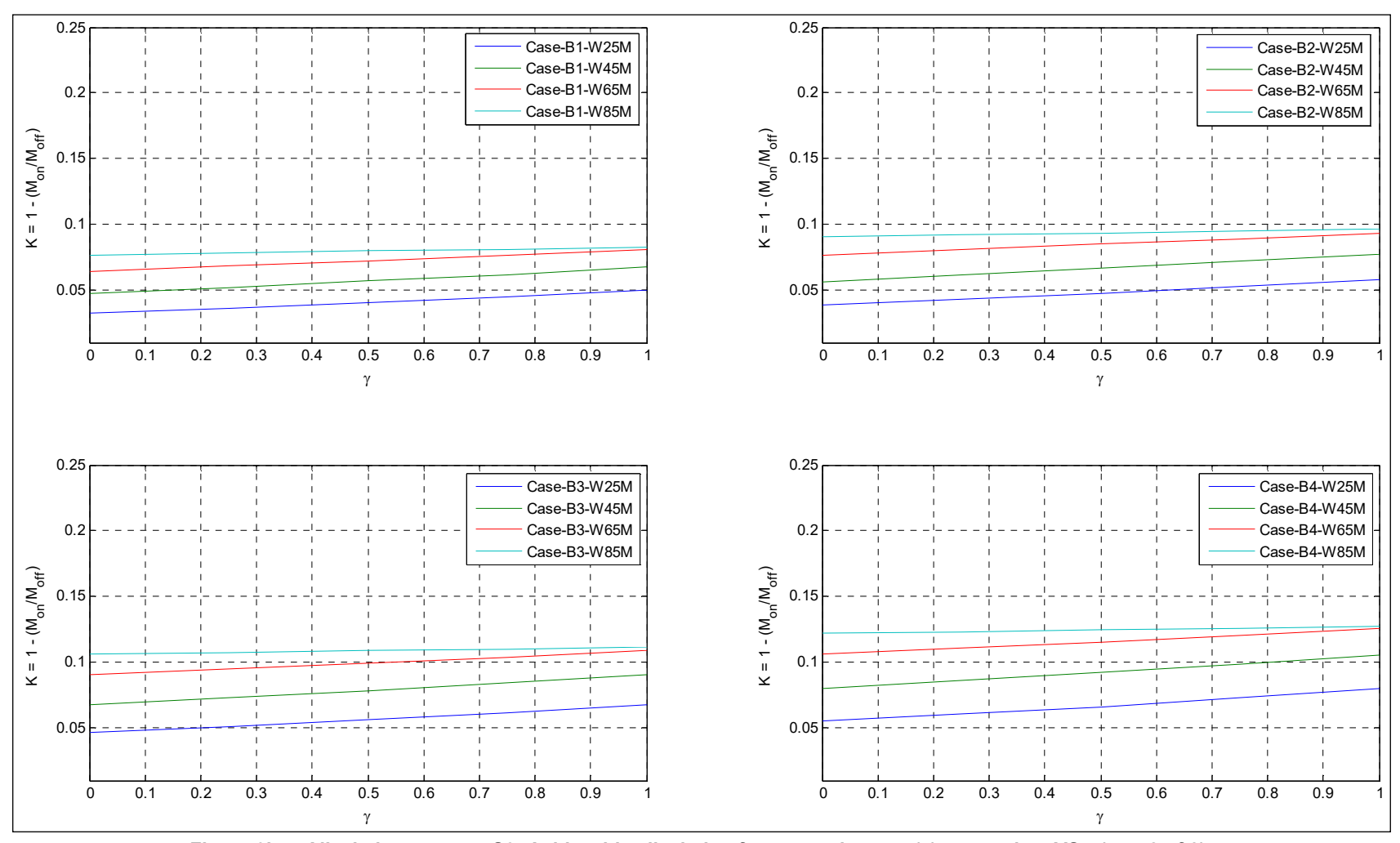


Figure 9b - Alleviation strategy S3: Achievable alleviation factors under eq.s (7) constraints VS γ (part 2 of 2).

6. Effects of load alleviation strategies on wing structure and aircraft aeroelastic stability

Based on the results presented in paragraph 5, trade-off studies on the effects induced by load alleviation strategies on wing structure and aircraft aeroelastic stability were conducted only for strategies S1 and S3.

Configuration cases A4 and A4_W65M (Table 4, paragraph 3) were used as reference for the alleviator's geometrical settings related to strategies S1 and S3 respectively.

The effects were evaluated by investigating the trends of relevant structural parameters with respect to variations in the load alleviation factor K; a step-by-step (iterative) procedure was implemented for this purpose.

Step 1 - Definition of A/C baseline aeroelastic model

The baseline wing structure was sized by adopting elementary methods from literature [7]-[8] and on the base of assumptions regarding:

- wing box layout and material;
- wing box elements contributes in bending moment, shear and torque moment absorption;
- desired safety margins along wing structural components.

The reference solicitations (bending/torque moments, shears) for the design of the baseline wing structure were obtained by integrating the ultimate aerodynamic loads arising at the rigid A/C trim condition of Table 6 and in absence of load alleviation.

Once the baseline wing structure was sized, the baseline aeroelastic model of the aircraft was set up by performing the following actions:

- generation of A/C stick-model for normal modes evaluation;
- generation of matching model for the interpolation of normal modes induced displacements on A/C aerodynamic lattice.

More specifically, a beam-equivalent model was generated for the wing box, accounting for the stiffness and inertial contributions of the leading edge. Additional lumped masses were introduced to consider the inertial contributions of the trailing edge and winglet (for CASE A4 W65M only).

A master node was positioned in the aircraft symmetry plane and loaded with a lumped mass M_0 and a lumped mass inertia $I_{0,YY}$ around the pitch axis Y, to properly include the inertial contributions of the fuselage and horizontal tail.

The values of lumped mass/inertia and its were calculated according to the overall aircraft weight and center of gravity position reported in Table 6 – paragraph 5 (A/C MTOW=40000 Kg, x_{cg} @ 21% of MAC. $I_{0,YY}$ was obtained based on the value of M_0 using similarity with existing aircraft in the same category as the reference one.

The inner node of the wing stick model was rigidly connected to the master node. For aero-structural matching purposes, supporting nodes were placed at the corner points defining the aerodynamic panels of the horizontal tail and winglet (CASE_A4_W65M only). Support nodes on the horizontal tail were rigidly connected to the master node, while those on the winglet were rigidly connected to the outer node of the wing stick model.

The matching model for the interpolation of normal modes on the aircraft aerodynamic lattice was obtained using appropriate linear and surface spline functions referred to both support and structural nodes. The aerodynamic lattices introduced in paragraph 4 were used for the evaluation of the generalized aerodynamic forces through the Doublet Lattice Method (DLM) [9].

The aeroelastic models generated for the configuration A4 and A4_W65M have been sketched in the next figure.

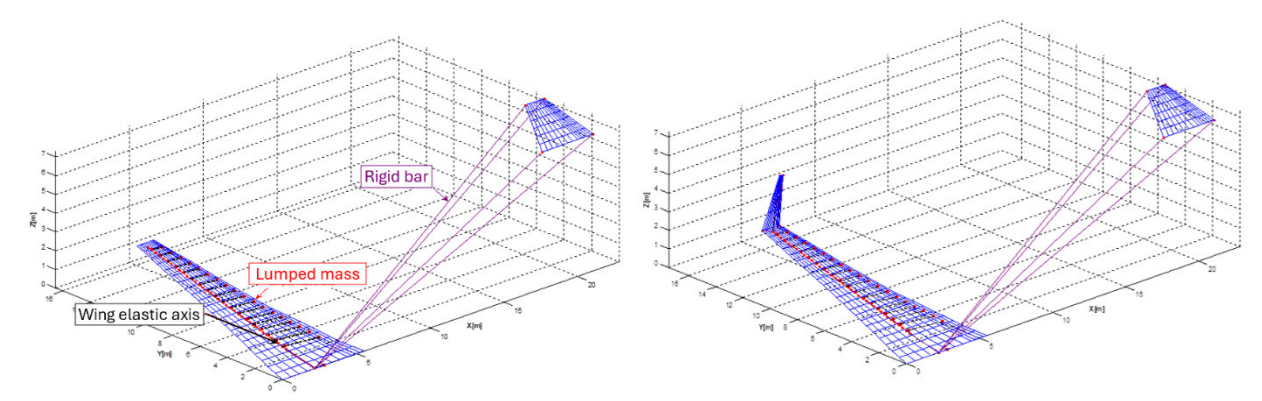


Figure 10 - Aeroelastic model: Case_A4 (left), Case_A4_W65M (right).

<u>Step 2</u> - Evaluation of trimmed solicitations on the baseline elastic wing at an alleviation factor Ki, and wing structure re-sizing

The baseline aircraft aeroelastic model was used to evaluate the elastic aircraft trim angles and wing load distribution related to the symmetric maneuver parameters of Table 6 – paragraph 5, with an alleviation factor K=K_i.

The wing structure was then re-sized based on the alleviated load distribution.

The re-sizing of the wing structure was carried out following an *iso-stress* approach [8], ensuring that the stress levels induced by alleviated loads on the resized structure were practically equal to those induced by non-alleviated loads on the baseline structure.

This approach led to two important implications:

- 1. The resized structure was able to withstand the respective (alleviated) loads with the same safety margins as the baseline structure subjected to non-alleviated loads.
- 2. As K_i increases, the resized structure becomes <u>reasonably</u> lighter and more flexible than the baseline structure.

<u>Step 3</u> - Evaluation of flutter speed using the A/C aeroelastic model based on the re-sized wing structure

Based on the resized wing structure from the previous step, a new aeroelastic model was generated for the aircraft, and flutter speeds were evaluated. Step 2 and Step 3 were repeated for different values of K (K_i), covering the ranges [0:0.2] for CASE_A4 and [0:0.25] for CASE_A4_W65M. The difference in K ranges is due to the different maximum alleviation factors obtainable for the investigated cases (see Figures 7 and 9, paragraph 5).

Figure 11 illustrates a flow chart of the iterative process and provides indications on the main parameters used to define the sensitivity curves for evaluating the effects of load alleviation on wing structure and aircraft aeroelastic stability.

The sensitivity curves obtained for the elastic trim angles versus the alleviation factor are presented in Figures 12 and 13 for cases A4 and A4_W6M, respectively. Figures 14 and 15 show the solicitations on the wing along the wingspan for different values of K and γ (where applicable). Finally, Figure 16 depicts the effects of load alleviation on the mass of the wing structures.

Based on these diagrams and the assumptions under which they were obtained, the following considerations can be made regarding the investigated alleviation strategies

- With an equal bending moment alleviation factor at the wing root, if the gear ratio (γ) is properly chosen, the alleviation strategy using ailerons and movable winglet surfaces (strategy S3) results in lower trim angles compared to the strategy using ailerons only (strategy S1).
- As a consequence of point 1, higher alleviation factors can be achieved with strategy S3 for the same aileron deflection.
- For the same alleviation factor, torque moments along the wing structure are greater when

TRADE OFF STUDIES ON WING MANEUVER LOAD ALLEVIATION STRATEGIES BASED ON AILERONS AND WINGLETS MOVABLE SURFACES strategy S3 is adopted.

 Rational resizing of the wing structure under alleviated loads leads to more significant mass reductions with strategy S3.

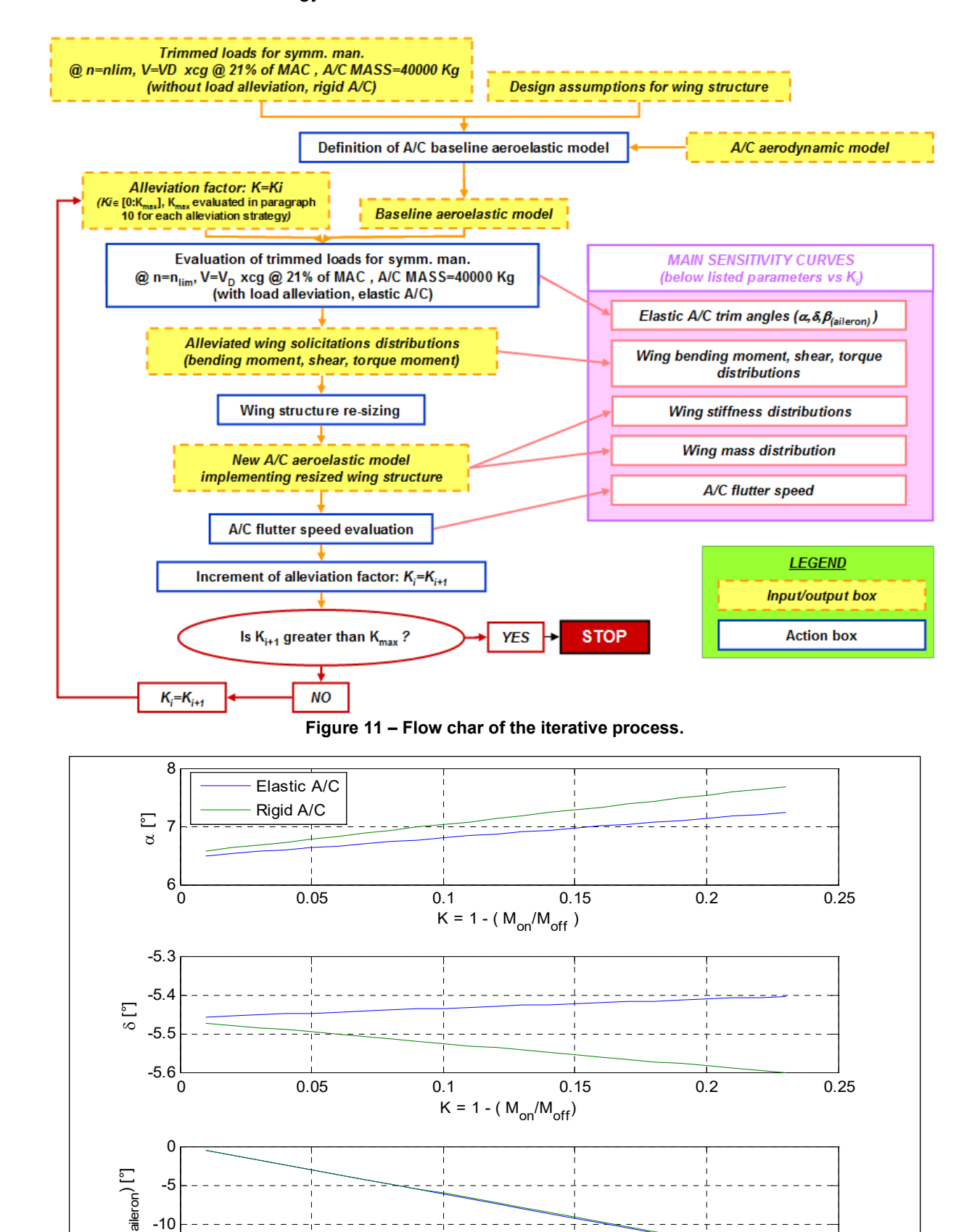


Figure 12 – CASE_A4: rigid and elastic A/C trim angles in presence of load alleviation.

 $K = 1 - (M_{on}/M_{off})$

0.2

0.25

0.1

-15

0.05

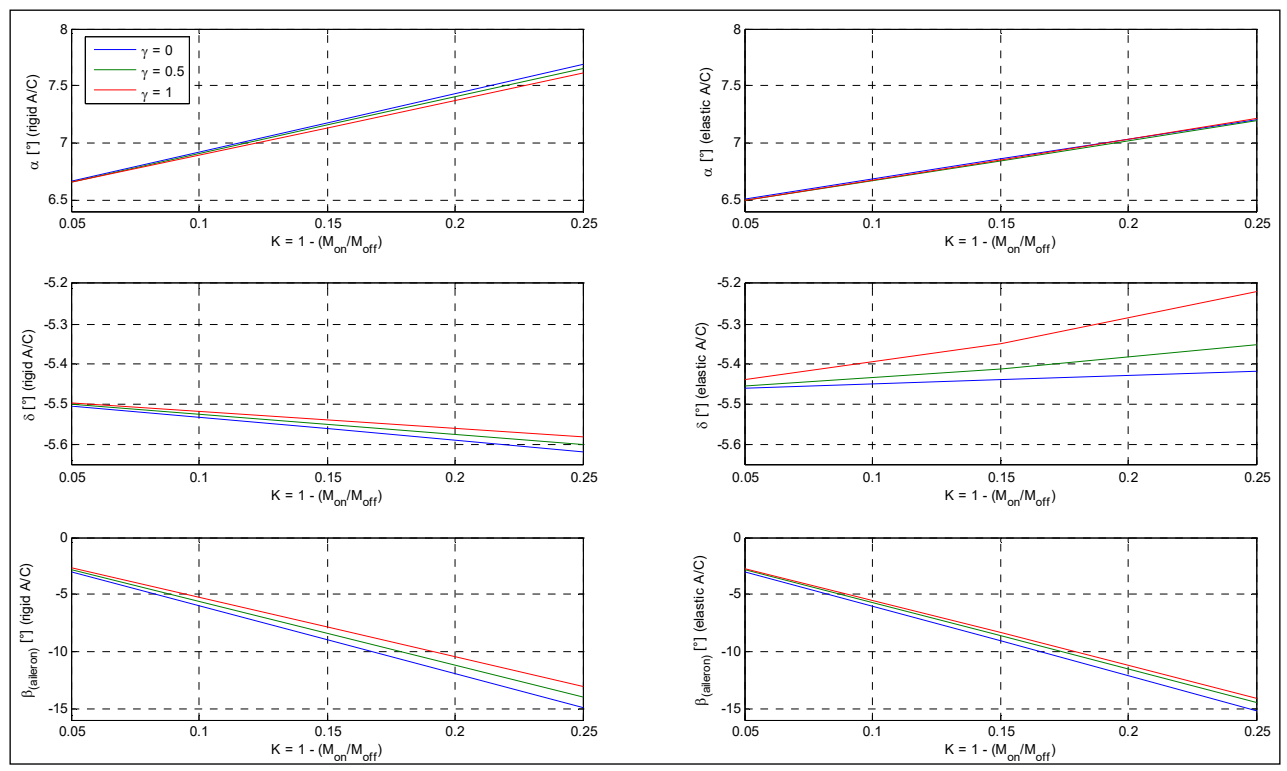


Figure 13 – CASE_A4_W65M: rigid and elastic A/C trim angles in presence of load alleviation.

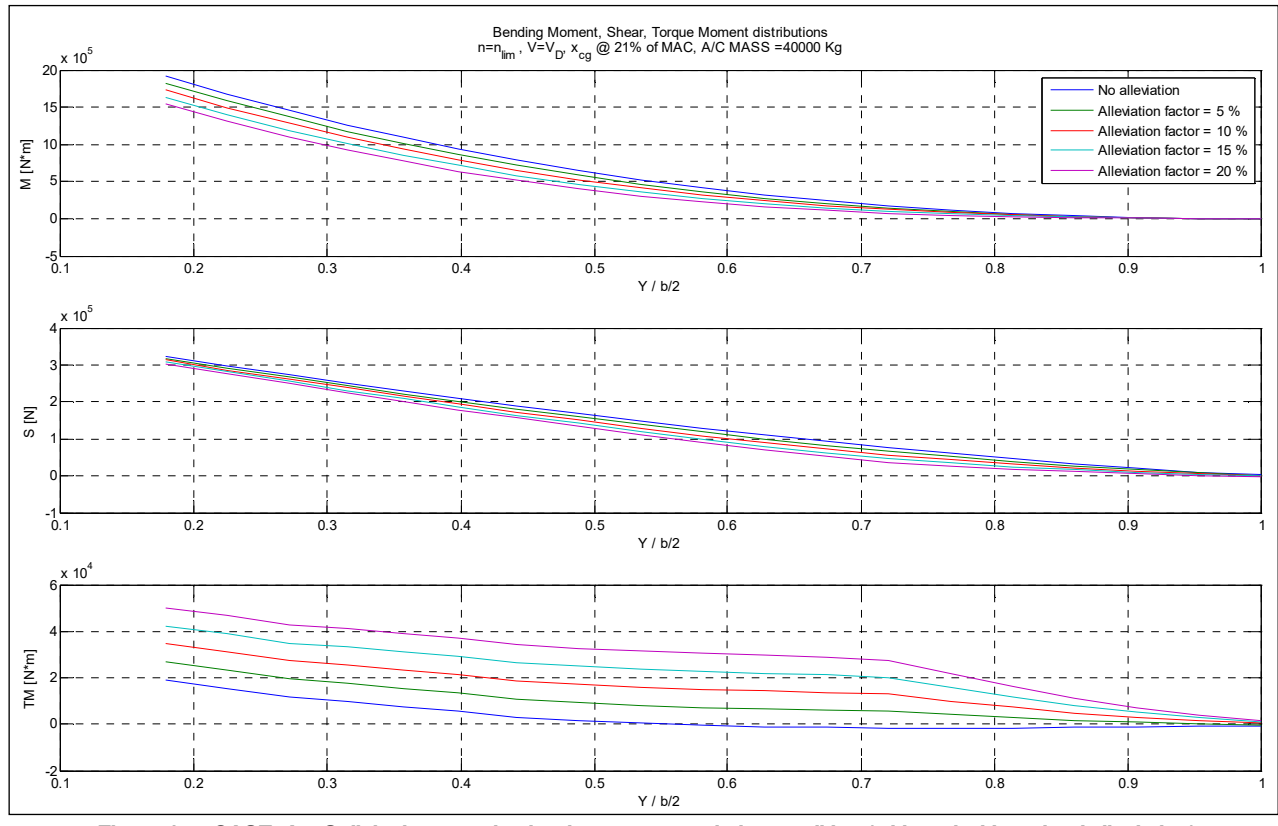


Figure 14 - CASE_A4: Solicitations on elastic wing at assumed trim condition (with and without load alleviation).

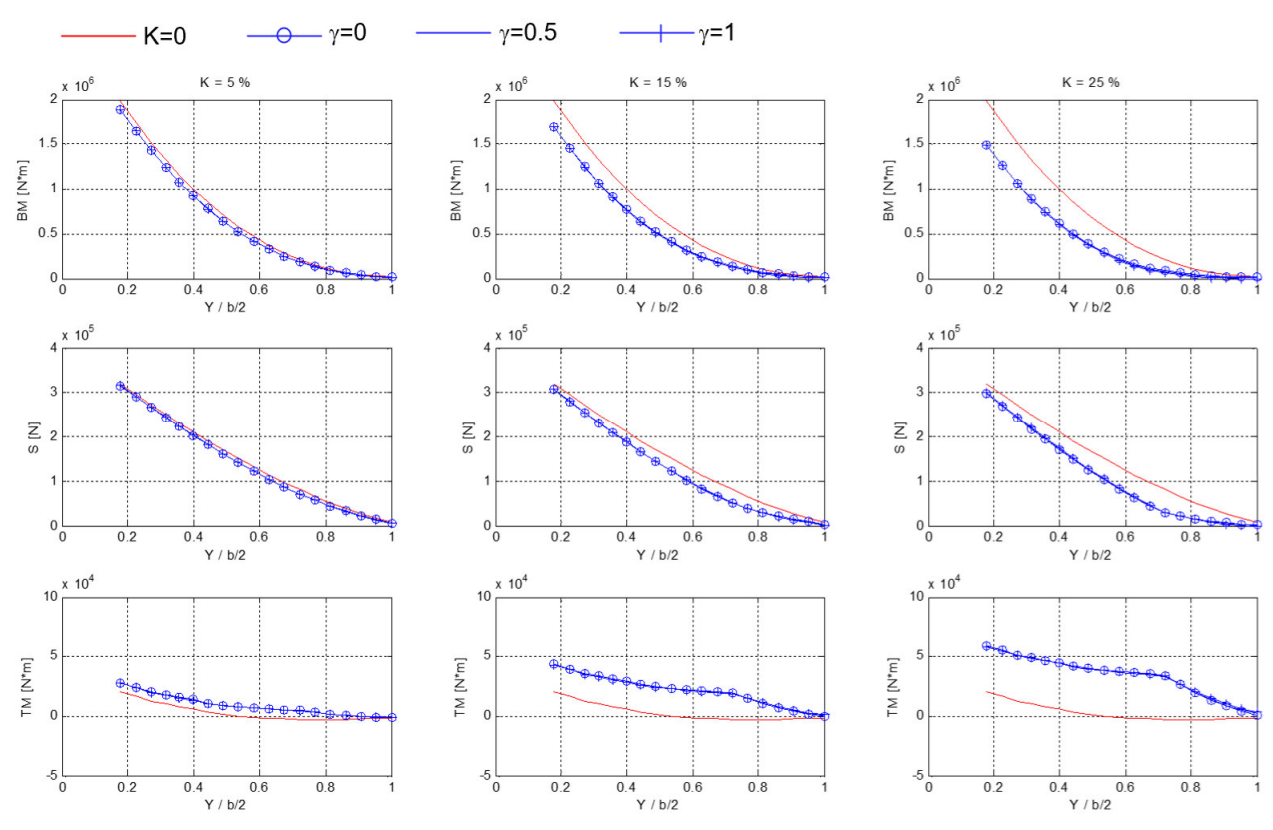


Figure 15 - CASE_A4_W65M: Solicitations on elastic wing at assumed trim condition (with and without load alleviation).

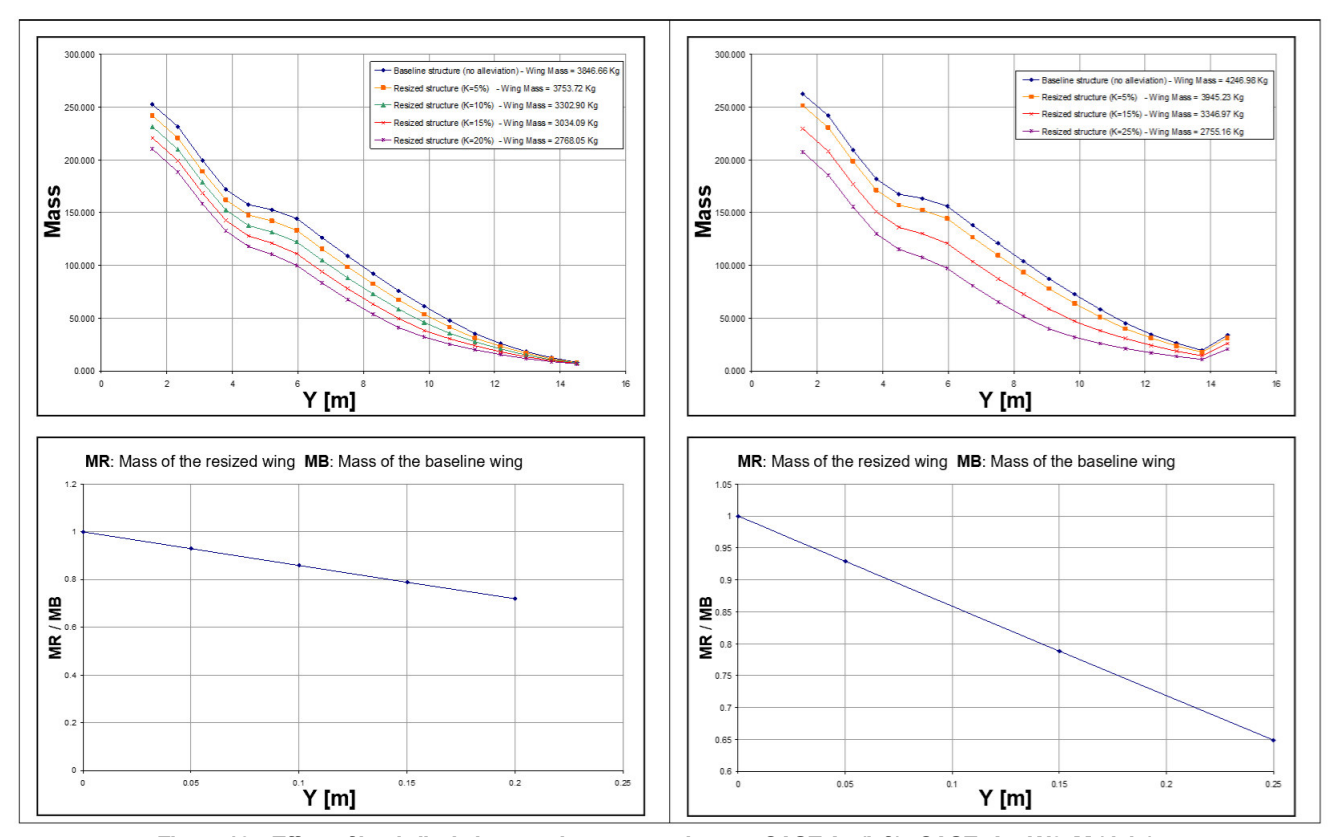


Figure 16 - Effect of load alleviation on wing structural mass: CASE A4 (left), CASE_A4_W65M (right).

Regarding wing aeroelastic stability, Figure 17 shows the flutter speed, V_F , (normalized with respect to the dive speed, V_D) for all the structural arrangements obtained for different values of the alleviation factor. It can be observed that as the alleviation factor increases, the flutter speeds related to CASE_A4_W65M come increasingly closer to the critical value imposed by airworthiness requirements (VF=1.2VD, [10], paragraph 629). This is primarily due to the decrease in wing torsion frequency induced by the presence of the winglet, while the bending frequency remains relatively unchanged compared to CASE_A4.

Two important conclusive considerations can therefore be made:

- From a flutter point of view, the alleviation strategy based on ailerons only (S1) is preferable to the one adopting both ailerons and movable winglet surfaces (S3).
- The greater achievable mass reductions shown in Figure 16 for strategy S3 are inevitably limited by the occurrence of flutter. To shift S3-related flutter speeds towards higher values, it may be necessary to increase the wing torsion frequency by making the wing structure stiffer and consequently heavier.

•

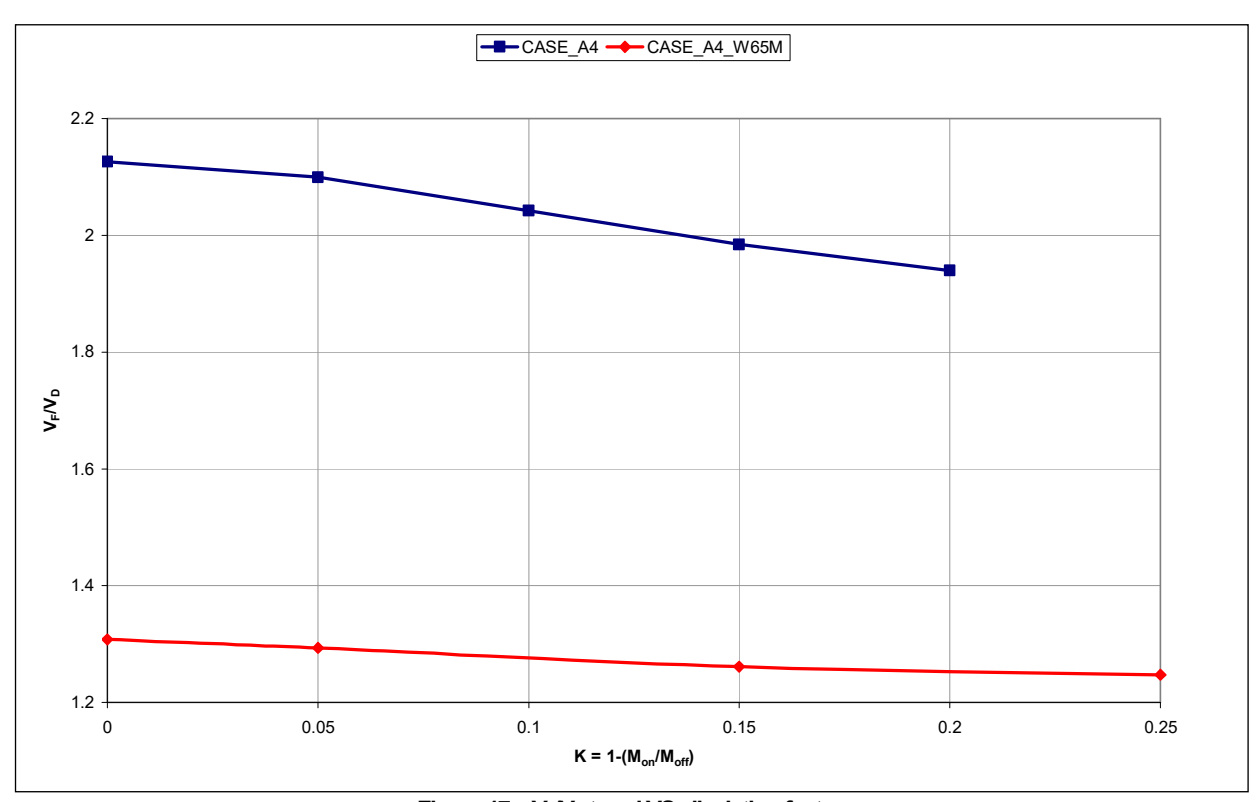


Figure 17 – V_F/V_D trend VS alleviation factor.

7. Conclusions

Referring to maneuver load alleviation strategies using ailerons and/or movable winglet surfaces as alleviators, sensitivity analyses have been carried out to:

- Investigate the efficacy of these strategies, for different geometrical settings of alleviator surfaces, in terms of achievable reductions in wing bending moment (and shear) at a significant design condition of the flight envelope.
- Investigate the implications of such reductions on wing structure sizing, and consequently on wing mass and aeroelastic behavior.

The investigated load alleviation strategies differ only in the type of movable surfaces used as alleviators; the alleviator control system has been assumed to be the same for each strategy and to operate based on the measured flight speed and aircraft load factor at the aircraft's center of gravity. Three different strategies have been analyzed:

- **S1** Alleviation strategy adopting only ailerons surfaces as alleviators;
- **S2** Alleviation strategy adopting winglets movable surfaces as alleviators;
- **S3** Combination of strategy S1 and S2: Both ailerons and movable winglet surfaces are used as alleviators. The deflection of the winglet movable surfaces is linked to the deflection of the ailerons according to a gear factor ratio γ.

With a reference operative condition for the load alleviation system defined in terms of aircraft design maneuver parameters, trade-off studies have been performed using a conceptual approach consisting of three consecutive phases:

- **Phase 1** Preliminary sensitivity analysis on the efficacy of alleviation strategies for various geometrical settings of alleviators (ailerons and/or movable winglet surfaces).
- **Phase 2** Identification of the optimal alleviator settings for each alleviation strategy.
- **Phase 3** Analysis of the effects induced by load alleviation strategies, integrating optimal alleviator settings, on wing structure and aeroelastic stability.

Based on the obtained results and the assumptions under which they were produced, the following main considerations can be made regarding the investigated alleviation strategies:

- 1. Strategy S2 is highly not recommendable due to its poor load alleviation performance.
- 2. With an equal bending moment alleviation factor at the wing root, if the gear ratio (γ) is properly chosen, strategy S3 leads to lower aircraft re-trim angles compared to strategy S1.
- 3. As a consequence of point 2, higher alleviation factors can be achieved with strategy S3 for the same aileron deflection.
- 4. For the same alleviation factor, torque moments along the wing structure are greater when strategy S3 is adopted.
- 5. For the same alleviation factor, rational wing-structure resizing under alleviated loads leads to more significant mass reductions with strategy S3
- 6. From a flutter perspective, the alleviation strategy based on ailerons only is preferable to the one using both ailerons and movable winglet surfaces
- 7. The mass reduction levels associated with strategy S3 must be inevitably limited by flutter considerations. For strategy S3, flutter occurs at speeds that are significantly lower than those related to strategy S1 and closer to the critical values imposed by airworthiness requirements. To shift S3 flutter speeds towards higher values, it may be necessary to increase wing torsion frequency by making the wing structure stiffer and consequently heavier.

Considering the observations for strategies S1 and S3, it is clear that each strategy has its own advantages and drawbacks.

Therefore, none of the investigated strategies can be considered absolutely better than the other. However, it can be concluded that strategy S3 may not be recommendable if winglets are to be installed solely for load alleviation purposes. At low and more practicable alleviation factors (5%, 10%), strategy S3 provides marginally greater benefits than strategy S1. However, the drawbacks associated with strategy S3 are much more significant than those of strategy S1 in terms of aircraft flutter behavior and the increased complications that may affect the alleviator control system design.

8. Contact Author Email Address

For any additional information on the contents of this paper, please contact: rosario.pecora@unina.it

9. Copyright Statement

The authors confirm that they, and/or their company or organization, hold copyright on all of the original material included in this paper. The authors also confirm that they have obtained permission, from the copyright holder of any third party material included in this paper, to publish it as part of their paper. The authors confirm that they give permission, or have obtained permission from the copyright holder of this paper, for the publication and distribution of this paper as part of the ICAS proceedings or as individual off-prints from the proceedings.

10. Acknowledgments

The authors wish to express their gratitude to the European Commission for providing the funding that made this research possible within the JTI-Clean Sky Programme. Additionally, sincere thanks are extended to Leonardo Aircraft for their significant contributions to defining the aerodynamic and inertial configurations of the aircraft, which served as a reference for the trade-off studies addressed in this paper.

11. References

- [1] NASA Contractor Report 3164 Selected Advanced Aerodynamics and Active Control Technology Concepts Development on a Derivative B-747 Aircraft, 1980 (open access).
- [2] McRuer D T, Graham D, Ashkenas I. *Aircraft Dynamics and Automatic Control*, Princeton Legacy Library, 2017.
- [3] Ravindra V J. *Flight Vehicle System Identification: A Time-domain Methodology*, American Institute of Aeronautics, 2nd edition, March 2015.
- [4] Stevens B L, Lewis F L, Johnson E N. Aircraft control and simulation, Wiley, 2015.
- [5] Web site: www.clean-aviation.eu
- [6] Kuethe A M, Chow C Y. Foundations of Aerodynamics-Bases of Aerodynamic Design, Wiley, 1986.
- [7] Bruhn E F. Analysis and Design of Flight Vehicle Structures, Tri State Offset Company, 1973.
- [8] Pecora R, Amoroso F, Lecce L. *Effectiveness of wing twist morphing in roll control*, Journal of Aircraft, Vol. 49(6), pp. 666–1674, 2012.
- [9] Broadbent E G. *Flutter and Response Calculations in Practice*, AGARD Manual on Aeroelasticity, Vol.3, NASA, 1963.
- [10] European Aviation Safety Agency, Certification Specifications and Acceptable Means of Compliance for Large Aeroplanes CS-25, Amendment 11, July 2011.